# REDUCED-ORDER MODELS FOR DAMPED GEOMETRICALLY NON-LINEAR VIBRATIONS OF THIN SHELLS VIA REAL NORMAL FORM

**Cyril Touzé[(1)], Marco Amabili[(2)], Olivier Thomas[(3)].**

(1) ENSTA-UME, Unité de Mécanique, Chemin de la Hunière, 91761 Palaiseau Cedex, France, *cyril.touze@ensta.fr*
(2) Dipartimento di Ingegneria Industriale, Università di Parma, Parco Area delle Scienze 181/A, Parma, 43100, Italy, *marco.amabili@unipr.it*
(3) CNAM, LMSSC, Laboratoire de Mécanique des structures et systèmes couplés, 2 rue Conté, 75003 Paris, France, *olivier.thomas@cnam.fr*

**Abstract:** *Reduced-order models for a general class of non-linear oscillators with viscous damping, quadratic and cubic non-linearities, are derived thanks to a real normal form procedure. A special emphasis is put on the treatment of the damping terms, and its effect on the normal dynamics. In particular, it is demonstrated that the type of non-linearity (hardening/softening behaviour) depends on damping. The methodology is then applied for reducing the non-linear dynamics exhibited by a circular cylindrical shell, hamonically excited in the spectral neighbourhood of the natural frequency of an asymmetric mode. The approximation, which consists in using time-invariant manifold instead of computing an accurate time-dependent one, is discussed. The results show that the method is efficient for producing accurate reduced-order models without a special need for intensive numerical computations. Validity limits of the approximation is then assessed by using the amplitude of the forcing as bifurcation parameter. Finally, the method is compared to the Proper Orthogonal Decomposition method (POD).*

## 1 Introduction

Large amplitude vibrations of thin shells give rise to typical phenomena that are activated by the geometrically non-linear terms in the equations of motion. The main problem associated with the analysis of these non-linear regimes is connected to the large dimension of the phase space, so that usual methods such as Galerkin projection onto the natural modes basis leads to a huge computational effort in order to derive the salient features of the motion. However, the complexity often consists in the curved geometry of the phase space, instead of being in the dynamics itself. Reduction methods, based on the idea of *non-linear normal modes* (NNMs), are specifically designed in order to include this geometrical complexity in the definition of an invariant manifold [1, 2, 3]. In a series of paper, Shaw, Pierre and coworkers use the technique provided by the center manifold theorem in order to reduce the original problem by projecting them onto a low-dimensional invariant manifold that catches the most important features. The method is a priori not restricted to conservative problems, and can handle gyroscopic as well as damping terms [2]. However, very few studies by these authors take damping terms into account.

Normal form theory can also be used as an alternative to center manifold reduction. The real formulation, proposed in [3] for conservative systems, defines of a non-linear change of coordinates, allowing one to express the dynamics in an invariant-based span of the phase space. The main purpose of this study is to extend the results of [3] so that modal viscous damping can be taken into account. It will be realized thanks to a kind of parameter continuation of the conservative results versus the damping terms. This result is then used for derivation of reduced-order models (ROMs) for continuous structures subjected to external harmonic forcing, the time-dependent invariant manifold of the forced problem being approximated by the time-invariant manifold precedently computed.

The outline of the paper is as follows. In section 2, the normal form, up to order 3, is computed, and the approximation used to compute the ROMs for continuous forced structures, are discussed. In section 3, it is

shown that the type of non-linearity (hardening or softening behaviour), depends on the damping coefficients. This result is illustrated with a two degrees-of-freedom (dofs) system. Section 4 is devoted to the vibrations of a fluid-filled circular cylindrical shell with harmonic forcing. The NNM method is compared with the POD method, and its validity limits are assessed via numerical simulations.

# 2 Theoretical formulation

## 2.1 Framework

Large amplitude, geometrically non-linear vibrations of continuous structures such as thin shells are here considered. Due to the initial curvature in the middle surface of shells-like structure, dynamical equations, derived from Von Karman's strain-displacement relationships, contain both quadratic and cubic non-linear terms. It is here assumed that the partial differential equations (PDEs) of motion have been discretized, *e.g.* by projection onto the eigenmodes basis, so that the starting point of this study is an assembly of $N$ oscillators ($N$ being as large as wanted) with general quadratic and cubic polynomial nonlinearities. It reads: $\forall p = 1...N$:

$$\ddot{X}_p + \omega_p^2 X_p + 2\xi_p\omega_p\dot{X}_p + \sum_{i=1}^{N}\sum_{j\geq i}^{N} g_{ij}^p X_i X_j + \sum_{i=1}^{N}\sum_{j\geq i}^{N}\sum_{k\geq j}^{N} h_{ijk}^p X_i X_j X_k = 0, \tag{1}$$

where $X_p$ stands for the modal displacement associated to the $p^{\text{th}}$ eigenmode of eigenfrequency $\omega_p$. The coefficients $g_{ij}^p$ and $h_{ijk}^p$ arise from the projection of the non-linear terms of the PDE onto the linear modes. Modal viscous damping terms of the form $2\xi_p\omega_p\dot{X}_p$ have also been introduced.

## 2.2 Non-linear change of coordinates

A third-order asymptotic development is introduced, in a similar manner than what has already been done in the undamped case [3]. The guidelines of the computation are the following. First, it is assumed that no internal resonances between the eigenvalues are present (this assumption may be relaxed and its effect on the results is easily obtained, see [3] and section 4). Secondly, a real formulation is kept throughout the calculations, so that the normal form will be expressed with oscillators. This is contrary to the usual complex formulation used in normal form computations (see *e.g.* [4, 5, 6]), and have important consequences for structural systems. Finally, the velocity $Y_p = \dot{X}_p$ is used so as to set Eq. (1) into its first-order form.

The non-linear change of co-ordinates reads:

$$\begin{aligned} X_p =& R_p + \sum_{i=1}^{N}\sum_{j\geq i}^{N}(a_{ij}^p R_i R_j + b_{ij}^p S_i S_j) + \sum_{i=1}^{N}\sum_{j=1}^{N} c_{ij}^p R_i S_j + \sum_{i=1}^{N}\sum_{j\geq i}^{N}\sum_{k\geq j}^{N}\left(r_{ijk}^p R_i R_j R_k + s_{ijk}^p S_i S_j S_k\right) \\ &+ \sum_{i=1}^{N}\sum_{j=1}^{N}\sum_{k\geq j}^{N}\left(t_{ijk}^p S_i R_j R_k + u_{ijk}^p R_i S_j S_k\right), \end{aligned} \tag{2a}$$

$$\begin{aligned} Y_p =& S_p + \sum_{i=1}^{N}\sum_{j\geq i}^{N}(\alpha_{ij}^p R_i R_j + \beta_{ij}^p S_i S_j) + \sum_{i=1}^{N}\sum_{j=1}^{N}\gamma_{ij}^p R_i S_j + \sum_{i=1}^{N}\sum_{j\geq i}^{N}\sum_{k\geq j}^{N}\left(\lambda_{ijk}^p R_i R_j R_k + \mu_{ijk}^p S_i S_j S_k\right) \\ &+ \sum_{i=1}^{N}\sum_{j=1}^{N}\sum_{k\geq j}^{N}\left(\nu_{ijk}^p S_i R_j R_k + \zeta_{ijk}^p R_i S_j S_k\right). \end{aligned} \tag{2b}$$

The full expressions of the introduced coefficients are not reported here for the sake of brevity. The interested reader can find them in [7]. This non-linear change of coordinates leads to cancellation of all the quadratic terms in the original dynamics, as these terms are non-resonant as long as no internal resonance relationship exists. On the other hand, a number of the cubic coefficients introduced in Eq. (2) vanish since they correspond to resonant cubic terms, which finally stay in the normal form. The normal dynamics can thus be

explicitely written: $\forall p = 1...N$ :

$$\begin{aligned}
&\ddot{R}_p + \omega_p^2 R_p + 2\xi_p\omega_p S_p + \left(h^p_{ppp} + A^p_{ppp}\right) R_p^3 + B^p_{ppp} R_p S_p^2 + C^p_{ppp} R_p^2 S_p \\
&+ R_p \Bigg[ \sum_{j>p}^{N} \left[ (h^p_{pjj} + A^p_{pjj} + A^p_{jpj}) R_j^2 + B^p_{pjj} S_j^2 + (C^p_{pjj} + C^p_{jpj}) R_j S_j \right] \\
&\quad + \sum_{i<p} \left[ (h^p_{iip} + A^p_{iip} + A^p_{pii}) R_i^2 + B^p_{pii} S_i^2 + (C^p_{pii} + C^p_{ipi}) R_i S_i \right] \Bigg] \\
&\quad + S_p \Bigg[ \sum_{j>p}^{N} \left( B^p_{jpj} R_j S_j + C^p_{jjp} R_j^2 \right) + \sum_{i<p} \left( B^p_{iip} R_i S_i + C^p_{iip} R_i^2 \right) \Bigg] = 0.
\end{aligned} \tag{3}$$

The coefficients $(A^p_{ijk},\ B^p_{ijk},\ C^p_{ijk})$ arise from the cancellation of the quadratic terms, and reads:

$$A^p_{ijk} = \sum_{l\geq i}^{N} g^p_{il} a^l_{jk} + \sum_{l\leq i} g^p_{li} a^l_{jk}, \tag{4a}$$

$$B^p_{ijk} = \sum_{l\geq i}^{N} g^p_{il} b^l_{jk} + \sum_{l\leq i} g^p_{li} b^l_{jk}, \tag{4b}$$

$$C^p_{ijk} = \sum_{l\geq i}^{N} g^p_{il} c^l_{jk} + \sum_{l\leq i} g^p_{li} c^l_{jk}. \tag{4c}$$

### 2.3 Reduced-order models

The dynamics, written with the introduced co-ordinates $(R_p, S_p)$ (non-linearly related to the initial modal coordinates), is now expressed within a curved invariant-based span of the phase space. Reduced-order models (ROMs) are constructed by simply selecting the master coordinates, and setting all others to zero. Thanks to the invariance property, these truncations may not produce erroneous results, since actual motions of the complete phase space will be computed with the reduced equations. In the conservative case, it has already been demonstrated in [3] that keeping a single NNM allows prediction of the correct type of non-linearity, whereas keeping a single linear mode may produce erroneous results.

As a consequence of the behaviour of the $(A^p_{ijk},\ B^p_{ijk},\ C^p_{ijk})$ terms with respect to the damping, a first-order damping development (limited to $\mathcal{O}(\xi_i)$ terms for lightly damped systems) shows that only $C^p_{ijk}$ is affected. For higher values of the damping, the three coefficients are affected, see section 3 where the focus is set on the variations of coefficients $(A^p_{ijk},\ B^p_{ijk})$, which govern the type of non-linearity. The main effect of keeping the linear damping terms in the normal form computation is the occurrence of $C^p_{ijk}$, which gathers them together so as to define a more precise decay of energy along the invariant manifolds. These new terms may be interpreted as non-linear dampers since they are linked to dynamical monoms of the form $\{R_\flat R_\flat \dot{R}_\flat\}_{\flat=i,j,p}$.

Application of the proposed ROMs to real situations leads to consider external forces applied to the structure. In this study, the ROM will be obtained by adding the external force directly to the normal form. The main advantage is that the calculation derived in section 2.2 is intrinsical to the structure, whereas rigorous computations including the external force must be done for each type of forcing studied. Secondly, the perturbation brought by the external force onto the normal form is at least a second-order effect [8].

Finally, real normal form theory allows derivation of simple ROMs with the main advantage that no specific numerical effort is needed. All the computations presented in the paper are immediate on a standard computer. However, two approximations are used. First, the normal form is computed via an asymptotic development, so that a validity limit, in terms of amplitude of vibration, exists. Secondly, when external forces are taken into account, the time-dependent manifold is approximated by the time-invariant NNMs computed

without external force. This second approximation sets a second limitation in terms of the amplitude of the forcing. In section 4, these validity limits will be numerically assessed, showing that the ROMs are valid for a very large range of parameters values.

# 3 Type of non-linearity

In this section, an important result is derived concerning the type of non-linearity for an assembly of oscillators defined by Eq (1). Thanks to real normal form theory, it is shown that the damping may have a strong influence on the type of non-linearity and may turn the behaviour from the hardening to the softening type.

## 3.1 Single NNM motion

A single master coordinate, say $p$, is retained in the normal form, Eq. (3). With a first-order perturbative method, the dependence of the frequency of free oscillations on the vibration amplitude may be expressed as: $\omega_{NL} = \omega_p(1 + T_p a^2)$, where $a$ is the vibration amplitude. Analytical expression of $T_p$ reads:

$$T_p = \frac{3(h^p_{ppp} + A^p_{ppp}) + \omega_p^2 B^p_{ppp}}{8\omega_p}. \tag{5}$$

Hardening behaviour is obtained for $T_p > 0$, whereas $T_p < 0$ implies softening behaviour. Since $A^p_{ppp}$ and $B^p_{ppp}$ gathers the conjugate influences of all the linear modes onto the NNM motion and depends on all the linear damping coefficients $\{\xi_i\}_{i\geq 1}$, this simple analytic formula shows that the type of non-linearity depends on the whole damping present in the structure, and not only on the conservative problem, as it is generally admitted. In order to study the effects of the neglected linear modes onto the type of non-linearity of the $p^{\text{th}}$ mode, a simple two-degrees-of-freedom (dofs) system is introduced in the next subsection.

## 3.2 A two dofs example

An extension of the simple mass-spring system selected in [3, 9] is here considered, where modal damping have been added to each equation. The dynamics reads:

$$\ddot{X}_1 + \omega_1^2 X_1 + 2\xi_1\omega_1\dot{X}_1 + \frac{\omega_1^2}{2}(3X_1^2 + X_2^2) + \omega_2^2 X_1 X_2 + \frac{\omega_1^2 + \omega_2^2}{2} X_1(X_1^2 + X_2^2) = 0 \tag{6a}$$

$$\ddot{X}_2 + \omega_2^2 X_2 + 2\xi_2\omega_2\dot{X}_2 + \frac{\omega_2^2}{2}(3X_2^2 + X_1^2) + \omega_1^2 X_1 X_2 + \frac{\omega_1^2 + \omega_2^2}{2} X_2(X_1^2 + X_2^2) = 0 \tag{6b}$$

All the subsequent analysis will consider the case where the first oscillator play the role of a central manifold, thus small values of $\xi_1$ will be selected. The second oscillator will play the role of a damped manifold, the dynamics of which will be enslaved in the first NNM. The effect of increasing values of $\xi_2$ is studied. As a consequence of the dependence of $A^1_{111}$ and $B^1_{111}$ on the damping terms $(\xi_1, \xi_2)$, the sign of $T_1$ may change for increasing $\xi_2$. This is illustrated for example in Fig. 1.

Another result is shown in Fig. 2, where the type of non-linearity is now represented as a function of $\omega_1$, and for different values of $\xi_2$. As already noticed by several studies [10, 11, 12, 13], a discontinuity is observed in these kind of non-linearity map, when a 2:1 internal resonance occurs (here we have $\omega_2 = 2\omega_1$). This is the logical effect of a small denominator, indicating that the calculation, realized under the assumption of no internal resonance, breaks down in the vicinity of the resonance. Here, it is shown that taking into account the whole damping of the structure smoothens the discontinuity. For increasing values of $\xi_2$, Figure 2 shows that the region of hardening behaviour after the 2:1 internal resonance decreases, and can even disappear, which happens here for $\xi_2 = 0.1$. From this study, it can be concluded that a careful prediction of the type of non-linearity must include the damping in the analysis. Further analysis on this point may be found in [7], where it is concluded that the effect of damping is generally to enhance and favour the softening behaviour.

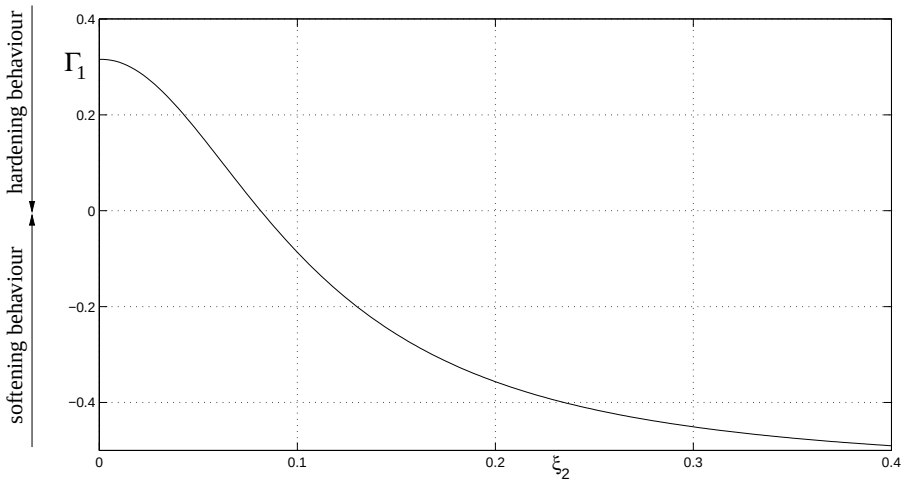


Figure 1: Type of non-linearity $T_1$, defined by Eq. (5), for increasing values of $\xi_2$. The behaviour turns from hardening to softening type for $\xi_2 = 0.081$. Other selected values are: $\omega_1 = 3$, $\omega_2 = 5.4$, and $\xi_1 = 0.001$.

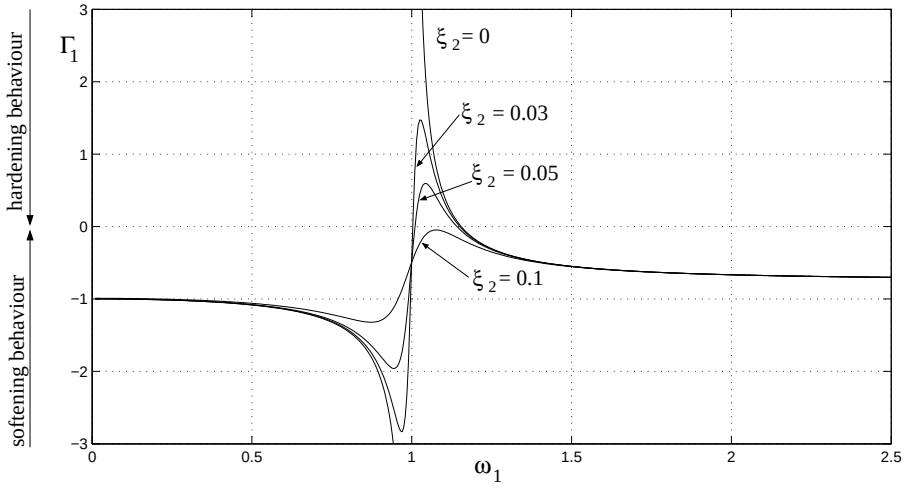


Figure 2: Type of non-linearity for different values of $\xi_2$, illustrating the fact that the discontinuity at the 2:1 internal resonance is smoothened by increasing the damping of the slave oscillator. $\omega_2 = 2$ and $\xi_1 = 0.001$.

# 4 Non-linear vibrations of circular cylindrical shells

## 4.1 Equations of motion

A water-filled perfect circular cylindrical shell, simply supported, and harmonically excited in the neighbourhood of the fundamental frequency, is selected in order to derive a NNM-based ROM for a continuous structure. A detailed discussion on the model can be found in [14, 15], so that only the important results with regard to the reduction process, are recalled. Donnell's non-linear shallow-shell theory is used to take into account large amplitude motions, so that in-plane inertia, transverse shear deformation and rotary inertia are neglected. The equation of motion for the transverse deflection $w(x, \theta, t)$ writes:

$$D\nabla^4 w + ch\dot{w} + \rho h\ddot{w} = f - p + \frac{1}{R}\frac{\partial^2 F}{\partial x^2} + \frac{1}{R^2}\left[\frac{\partial^2 F}{\partial \theta^2}\frac{\partial^2 w}{\partial x^2} - 2\frac{\partial^2 F}{\partial x \partial \theta}\frac{\partial^2 w}{\partial x \partial \theta} + \frac{\partial^2 F}{\partial x^2}\frac{\partial^2 w}{\partial \theta^2}\right], \qquad (7)$$

where $D$ is the flexural rigidity, $E$ Young's modulus, $\nu$ Poisson's ratio, $h$ the shell thickness, $R$ the mean shell radius, $\rho$ the mass density, $c$ the coefficient of viscous damping, $p$ the radial pressure applied to the surface of

the shell by the contained fluid, and $f$ is a point excitation, located at $(\tilde{\theta}, \tilde{x})$ :

$$f = \tilde{f}\delta(R\theta - R\tilde{\theta})\delta(x - \tilde{x})\cos(\omega t). \tag{8}$$

$F$ is the usual Airy stress function, which satisfies the following compatibility equation:

$$\frac{1}{Eh}\nabla^4 F = -\frac{1}{R}\frac{\partial^2 w}{\partial x^2} + \left[\left(\frac{\partial^2 w}{R\partial x \partial\theta}\right)^2 - \frac{\partial^2 w}{\partial x^2}\frac{\partial^2 w}{R^2\partial\theta^2}\right]. \tag{9}$$

A circumferentially closed circular cylindrical shell of length $L$ is considered. Mathematical expressions of boundary conditions are given in [14, 15]. The contained fluid is assumed to be incompressible, inviscid and irrotational. The expression of $p$, which describes the fluid-structure interaction, is given in [14].

The PDE of motion is discretized by projection onto the natural modes basis. The reference solution, whose convergence has been carefully verified in [12, 14], is computed by keeping 16 natural modes. The transverse deflection is thus expanded via:

$$w(x,\theta,t) = \sum_{\substack{m=1\\k=1}}^{3} [A_{m,kn}(t)\cos(kn\theta) + B_{m,kn}(t)\sin(kn\theta)]\sin(\lambda_m x) + \sum_{m=1}^{4} A_{(2m-1),0}(t)\sin(\lambda_{(2m-1)}x), \tag{10}$$

where $n$ is the number of circumferential waves, $m$ the number of longitudinal half-waves (for symmetry reasons, only odd values are retained), $\lambda_m = m\pi/L$; $A_{m,n}(t)$ and $B_{m,n}(t)$ are the generalized coordinates. By use of the Galerkin method, 16 second-order differential equations are obtained. They are in the form of the general equations used as the starting point of this study, Eq. (1), by simply adjusting the $X_p$ and postulating modal damping.

The reference solution is obtained for the following shell: $L = 520$ mm, $R = 149.4$ mm, $h = 0.519$ mm, $E = 2.06.10^{11}$ Pa, $\rho = 7800$ kg.m$^{-3}$, $\rho_F = 1000$ kg.m$^{-3}$ (water-filled shell), and $\nu$ =0.3. The excitation frequency $\omega$ is set in the vicinity of the fundamental mode ($n$=5, $m$=1), whose eigenfrequency is 79.21 Hz. Modal damping $\xi_{1,n} = 0.0017$ is assumed. The harmonic point excitation is located at $\tilde{x} = L/2$ and $\tilde{\theta} = 0$, and two different magnitudes will be used to obtain numerically the frequency-response curves : 3N and 8N.

In the next subsections, two different ROMs will be used and compared. The first one is obtained with the real normal form procedure described in the precedent sections. The second one is obtained by application of the POD method. Detailed comments on the construction of the POD-based ROM are not provided here for the sake of brevity, the interested reader can find them in [15, 16].

## 4.2 Frequency-response curves

The response of the shell in the vicinity of an asymmetric mode is investigated. As a consequence of the rotational symmetry displayed by the shell, asymmetric modes appears by pairs, and 1:1 internal resonance exists between each pair of companion modes. Hence, the minimal model which could capture accurately the dynamics is composed of two NNMs, and is simply written from Eq. (3), by keeping the two master coordinates corresponding to the driven and the companion mode, and cancelling all the others.

The POD model is computed from time series obtained by direct time-integration of the full order model. A great care must be observed in the choice of these time series, as reported in [15]. The minimal model found is composed of three proper orthogonal modes (POMs), as any POD model with two POMs were unable to detect a crucial bifurcation point, leading to coupled solutions and travelling waves.

The frequency-response curves for excitation amplitude of 3 N are reported on Fig. 3. The reference solution is composed of two branches. The main branch corresponds to zero amplitude for the companion mode $B_{1,5}$, and has two pitchfork bifurcations (BP) at $\omega/\omega_{1,5}$= 0.9714 and at 1.0018, where the second branch appears. This new branch corresponds to participation of both $A_{1,5}$ and $B_{1,5}$, giving a travelling wave response. The second branch undergoes two Neimark-Sacker (torus) bifurcations (TR), at $\omega/\omega_{1,5}$= 0.9716 and 0.9949. Betwen these two values, amplitude-modulated (quasi-periodic) responses are found to exist. The two ROMs gives very satisfactorily results for this case. Both predict finely the bifurcations points, and

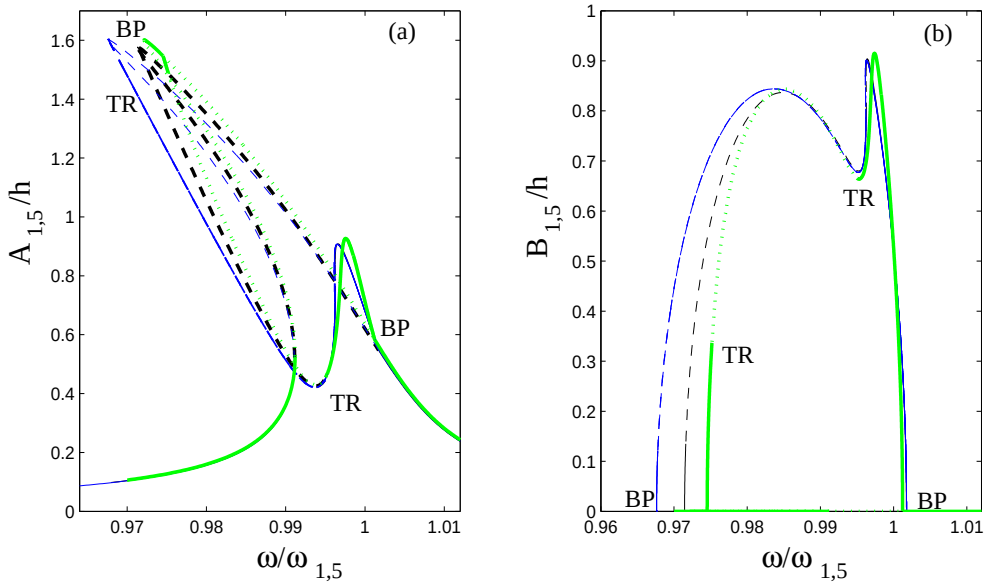


Figure 3: Frequency-response curves for (a): the driven mode $A_{1,5}$ and (b): the companion mode $B_{1,5}$, for the shell model, harmonically excited in the vicinity of $\omega_{1,5}$. Black line is the reference solution, computed with 16 eigenmodes. Green line is the POD solution computed by keeping three POD modes. Blue line is the NNM ROM, computed by keeping two NNMs. Stability is indicated with dotted and dash-dotted lines.

every solutions, as well as their stability type, are recovered. The only difference being that the NNM ROM needs only two dofs, whereas three POD modes have been necessary to recover the second branch.

The two ROMs have also been tested for a higher value of the forcing amplitude, which have been set at 8N: the responses are reported on Fig. 4, where the following comments are worth mentionable. First of

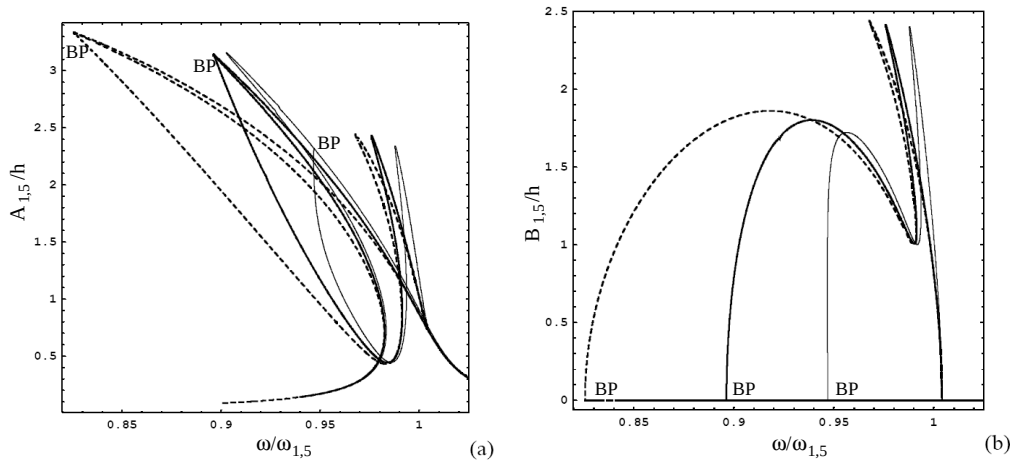


Figure 4: Frequency-response curves for (a): the driven mode $A_{1,5}$ and (b): the companion mode $B_{1,5}$, for the shell model, harmonically excited in the vicinity of $\omega_{1,5}$, excitation amplitude at 8N. Thick line : reference solution, thin line : POD solution, dashed line : NNM.

all, the POD model seems to behave better than the NNM model, as solution branches of the POD ROM are closer to the original solution than the solution branches provided by keeping 2 NNMs. However, the branch switching (BP) on the second branch predicted by the POD model are shifted to the right of the branch, hence overpredicting the range of stable periodic solutions, so that a slight change in the qualitative predictions are

given by the POD model. On the other hand, the qualitative predictions of the NNM-based ROM are still very good, but in this case the softening behaviour is overpredicted.

It can be observed here that the POD model could be improved by using a time response computed for excitation of 8 N to find the proper orthogonal modes; however it has been found more interesting here to investigate the robustness of a reduced order model to changes in the system parameters, so that the POD model built with the response at 3N was used here for excitation amplitude of 8N. On the other hand, the NNM model is built once and for all, and may not been changed when varying the amplitude of the forcing. The observed differences with the reference solution are the consequences of the two approximations used to build it: asymptotic development and time-invariant manifold.

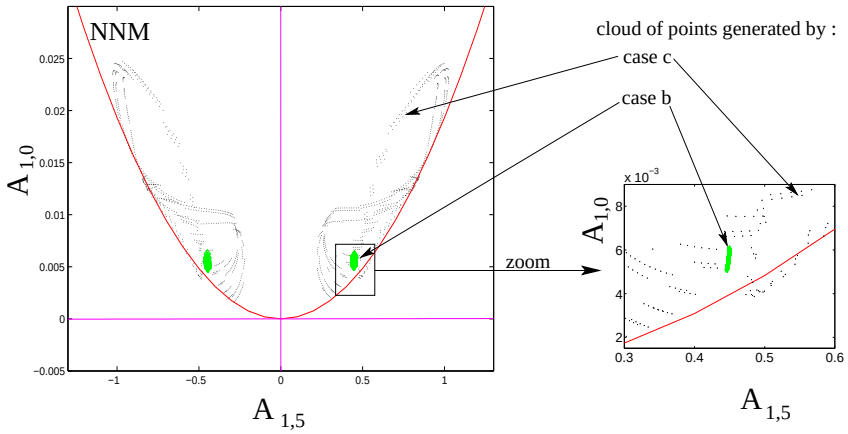


Figure 5: Poincaré section in $(A_{1,5},\ A_{1,0})$. Clouds of points : section of the orbits generated by case b (perdiodic coupled response) and case c (quasiperiodic coupled response). POD axis differs very few from the original x- and y-axis, whereas the cut of the 4-dimensional invariant manifold used to construct the NNM-based ROM goes right in-between the points.

In order to get a geometrical interpretation of the frequency-response curves shown in the precedent section, a Poincaré section of the 32-dimensional phase space is proposed in Fig. 5. Two clouds of points, corresponding to time series computed from the full-order model, are represented by points. The Poincaré section is the plane $(A_{1,5},\ A_{1,0})$, each point corresponding to a cut through that section. The first time series (case b) has been computed from a periodic coupled solution, whereas the second one (case c) corresponds to the quasiperiodic regime found on the second branch, and is exactly the time series that has been used to construct the POD model. This figure illustrates clearly why 3 POD modes are necessary to recover the dynamics: as a significant contribution onto the $A_{1,0}$ coordinate is found, the corresponding POD axis must be mandatory kept. This can also be connected to the fact that the POD method is linear, as it furniches the best orthogonal axis that contains most information. On the other hand, the NNM method is non-linear, and construct a curved invariant manifold to approximate the dynamics. That's why in this case, only 2 NNMs allows recovering the dynamics.

### 4.3 Bifurcation diagram with varying amplitude of forcing

The three models are now investigated for a fixed excitation frequency, and by using the excitation amplitude as bifurcation parameter. The objective are twofold: first to detect more complex behaviours and test the robustness of the reduced models over a wide range of variation where mutliple states are found to exist, from periodic to chaotic responses. Secondly, it is a way to find the validity limits of the asymptotic NNM, computed with two approximations, in terms of amplitude of vibrations and amplitude of forcing.

The result of the computation, for the ROM composed of 2 NNMs, is shown on Fig. 6. Direct numerical integration is performed with the Gear's BDF method, and has found to be very slow and difficult to obtain for

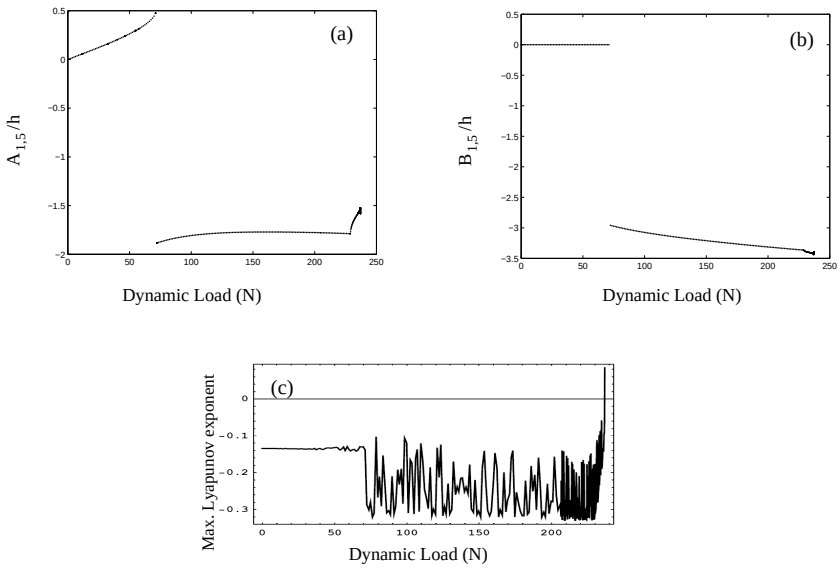


Figure 6: Bifurcation diagram of Poincaré maps and maximum Lyapunov exponent for the shell under increasing harmonic load with frequency $\omega$=0.92$\omega_{1,5}$ for the NNM ROM with two dofs. (a): generalized coordinate $A_{1,5}(t)$, driven mode. (b): generalized coordinate $B_{1,5}(t)$, companion mode. (c): maximum Lyapunov exponent.

large values of the forcing amplitude. More precisely, it has been found impossible to perform the integration over the right-end point shown in Fig. 6 at about 240 N. This indicates that the validity limit of the ROM is reached. For values of the forcing amplitude below 240 N, qualitative and quantitative comparison with the full-order model, is found to be reasonably good.

Results for the POD models are not reported here, the interested reader can find them in [16]. It shows that the model composed of 3 POD modes gives poor results, as compared to the original one, but without the problem mentioned before for the NNM model : integration was possible, but qualitative discrepancies were found. A model composed of 5 POD modes, with time series obtained in the chaotic regime, has been found to recover satisfactorily the main features of the bifurcation diagram [16].

# 5 Conclusion

A normal form procedure for an assembly of $N$ non-linear oscillators, including a non-conservative perturbation brought by a modal viscous damping term, has been derived. It allows construction of simple NNM reduced-order models, with applications to geometrically non-linear vibrations of structures, with the limitation that an asymptotic approach to the invariant manifold is given. With a second approximation, external forces can be taken into account, by using the time-invariant manifold constructed from the normal form procedure instead of the time-dependent ones.

With this methodology, a result concerning the influence of the damping on the type of non-linearity, has been obtained. It shows that the damping generally flavours the softening type non-linearity, and large values of damping of neglected modes may change the behaviour of the selected one from hardening to softening.

Finally, the method has been applied so as to derive ROMs of a fluid-filled circular cylindrical shell, harmonically excited in the neighbourhood of the fundamental mode. Numerical results shows that the NNM-based ROM gives perfect results for low values of forcing amplitude (3N of amplitude of excitation, which results in a displacement of approximately 1.5 times the thickness of the shell). For larger values (8N of amplitude of excitation, which results in a displacement of 3 times the thickness of the shell), results are still qualitatively in close agreement, with a slight overprediction of the softening type behaviour. The validity limit, in terms of amplitude of forcing, has been assessed with numerical integration: it has been found that

up to 240 N of excitation, the model was useable. This clearly points out that these reduced models, which are very easy to compute, without a special numerical effort, gives very satisfactorily results for a large range of parameters values, i.e. for vibration amplitude up to 3 times the thickness, and forcing amplitude up to 240 N.

Comparison with the POD method have also been drawn. The results can be interpreted as consequences of the way the models are built. POD method is in essence linear, so that for low amplitudes of forcing, a better reduction is provided by the NNM method, which is non-linear, and allows projection onto curved subspaces. The NNM method used here, relies on a local theory (normal form procedure), so that the obtained results are not valid everywhere. This is not the case for the POD method, which is global, and allows recovering the bifurcation diagrams with varying the force amplitude, provided a robust model (here with 5 POD modes), built in the chaotic regime, has been established. Further comparisons between the two methods with regard to the results presented in this paper are provided in [17].

## References


[1] S. W. Shaw and C. Pierre: Non-linear normal modes and invariant manifolds, *J. Sound Vib.* **150**(1), 170-173,1991.

[2] S. W. Shaw and C. Pierre: Normal modes for non-linear vibratory systems, *J. Sound Vib.* **164**(1), 85-124, 1993.

[3] C. Touzé, O. Thomas and A. Chaigne: Hardening/softening behaviour in non-linear oscillations of structural systems using non-linear normal modes, *J. Sound Vib.* **273**(1-2), 77-101, 2004.

[4] C. Elphick, E. Tirapegui, M.E. Brachet, P. Coullet and G. Iooss: A simple global characterization for normal forms of singular vector fields, *Physica D*, **29**, 95-127, 1987.

[5] L. Jézéquel and C. H. Lamarque. Analysis of non-linear dynamical systems by the normal form theory, *J. Sound. Vib.*, **149**(3), 429-459, 1991.

[6] A. H. Nayfeh: Method of Normal Forms, John Wiley & sons, New-York, 1993.

[7] C. Touzé and M. Amabili: Non-linear normal modes for damped geometrically non-linear systems: application to reduced-order modeling of harmonically forced structures, *J. Sound Vib.*, submitted, 2005.

[8] G. Iooss and M. Adelmeyer: Topics in bifurcation theory, World scientific, New-York, second edition, 1998.

[9] S. Bellizzi and R. Bouc: A new formulation for the existence and calculation of nonlinear normal modes, *J. Sound Vib.*, **287**(3), 545-569, 2005.

[10] G. Rega, W. Lacarbonara and A. H. Nayfeh: Reduction methods for nonlinear vibrations of spatially continuous systems with initial curvature, *Solid Mechanics and its applications*, **77**, 235-246, 2000.

[11] H. N. Arafat and A. H. Nayfeh: Non-linear responses of suspended cables to primary resonance excitation, *J. Sound. Vib.*, **266**, 325-354, 2003.

[12] F. Pellicano, M. Amabili and M. P. Païdoussis: Effect of the geometry on the non-linear vibration of circular cylindrical shells, *Int. J. Non-linear Mech.*, **37**, 1181-1198, 2002.

[13] C. Touzé and O. Thomas: Non-linear behaviour of free-edge shallow spherical shells: Effect of the geometry, *Int. J. Non-linear Mech.*, In press, 2006.

[14] M. Amabili: Theory and experiments for large-amplitude vibrations of empty and fluid-filled circular cylindrical shell with imperfections, *J. Sound Vib.*, **262**(4), 921-975, 2003.

[15] M. Amabili, A. Sarkar and M. P. Païdoussis: Reduced-order models for nonlinear vibrations of cylindrical shells via the proper orthogonal decomposition method, *J. Fluids Struct.*, **18**(2), 227-250, 2003.

[16] M. Amabili, A. Sarkar and M. P. Païdoussis: Chaotic vibrations of circular cylindrical shells: Galerkin versus reduced-order models via the proper orthogonal decomposition method, *J. Sound. Vib.*, **290**(3-5), 736-762, 2006.

[17] M. Amabili and C. Touzé: Reduced-order models for non-linear vibrations of circular cylindrical shells: comparison of POD and asymptotic Non-linear Normal Modes methods, *J. Fluids Struct.*, submitted, 2006.